

## REPORT DOCUMENTATION PAGE

Form Approved  
OMB No. 0704-0188

The public reporting burden for this collection of information is estimated to average 1 hour per response, including the time for reviewing instructions, searching existing data sources, gathering and maintaining the data needed, and completing and reviewing the collection of information. Send comments regarding this burden estimate or any other aspect of this collection of information, including suggestions for reducing the burden, to the Department of Defense, Executive Services and Communications Directorate (0704-0188). Respondents should be aware that notwithstanding any other provision of law, no person shall be subject to any penalty for failing to comply with a collection of information if it does not display a currently valid OMB control number.

PLEASE DO NOT RETURN YOUR FORM TO THE ABOVE ORGANIZATION.

|   |   |   |   |                                |  |
|---|---|---|---|--------------------------------|--|
| 1. REPORT DATE (DD-MM-YYYY)<br>07-19-2012   | 2. REPORT TYPE<br>Conference Proceeding | 3. DATES COVERED (From - To)  |   |                                |  |
| 4. TITLE AND SUBTITLE<br>What is Required to Model the Global Ocean Circulation?  |   | 5a. CONTRACT NUMBER   |   |                                |  |
|   |   | 5b. GRANT NUMBER  |   |                                |  |
|   |   | 5c. PROGRAM ELEMENT NUMBER<br>0602435N                              |   |                                |  |
| 6. AUTHOR(S)<br>James G.. Richman, Prasad G. Thoppil, Patrick J. Hogan and Alan J. Wallcraft  |   | 5d. PROJECT NUMBER  |   |                                |  |
|   |   | 5e. TASK NUMBER   |   |                                |  |
|   |   | 5f. WORK UNIT NUMBER<br>73-8677-01-5                                |   |                                |  |
| 7. PERFORMING ORGANIZATION NAME(S) AND ADDRESS(ES)<br>Naval Research Laboratory<br>Oceanography Division<br>Stennis Space Center, MS 39529-5004   |   | 8. PERFORMING ORGANIZATION<br>REPORT NUMBER<br>NRL/PP/7320--12-0721 |   |                                |  |
| 9. SPONSORING/MONITORING AGENCY NAME(S) AND ADDRESS(ES)<br>Office of Naval Research<br>One Liberty Center<br>875 North Randolph Street, Suite 1425<br>Arlington, VA 22203-1995  |   | 10. SPONSOR/MONITOR'S ACRONYM(S)<br>ONR                             |   |                                |  |
|   |   | 11. SPONSOR/MONITOR'S REPORT<br>NUMBER(S)                           |   |                                |  |
| 12. DISTRIBUTION/AVAILABILITY STATEMENT<br>Approved for public release, distribution is unlimited.<br><br>20120802046   |   |   |   |                                |  |
| 13. SUPPLEMENTARY NOTES   |   |   |   |                                |  |
| 14. ABSTRACT<br>Simulating and forecasting the circulation of the global ocean is a difficult task. The present generation of high-resolution ocean circulation models, with horizontal resolution of ~1/10, appears to be deficient in kinetic energy when compared with long-term observations. A series of near-twin experiments, using the global HYbrid Coordinate Ocean Model (HYCOM) with identical atmospheric forcing, but varying in horizontal resolution and assimilation of altimetric steric height anomalies, show significant improvement with a better representation of mesoscale eddies when compared to observations. For a 1/12.5 (~9 km) global model, the eddy kinetic energy (EKE) at the surface and abyss is low by ~21% and ~24%, respectively, compared to surface drifting buoys and deep current meters. Increasing the model resolution to 1/25 (~4.4 km) or injecting mesoscale eddies through the assimilation of surface observations in a 1/12.5 model increases the surface and abyssal EKE to levels consistent with observations. |   |   |   |                                |  |
| 15. SUBJECT TERMS<br>internal tides, ocean circulation modeling, data assimilation, Eddies and mesoscale processes  |   |   |   |                                |  |
| 16. SECURITY CLASSIFICATION OF:<br>a. REPORT<br>Unclassified  | b. ABSTRACT<br>Unclassified             | c. THIS PAGE<br>Unclassified  | 17. LIMITATION OF<br>ABSTRACT<br>UU                       | 18. NUMBER<br>OF<br>PAGES<br>7 | 19a. NAME OF RESPONSIBLE PERSON<br>James Richman |
|   |   |   | 19b. TELEPHONE NUMBER (Include area code)<br>228-688-4933 |                                |  |

## What is Required to Model the Global Ocean Circulation?

James G. Richman, Prasad G. Thoppil, Patrick J. Hogan, and Alan J. Wallcraft  
US Naval Research Laboratory, Oceanography Division (NRL-SSC), Stennis Space Center, MS  
[{james.richman, prasad.thoppil, pat.hogan, alan.wallcraft}@nrlssc.navy.mil](mailto:{james.richman, prasad.thoppil, pat.hogan, alan.wallcraft}@nrlssc.navy.mil)

### Abstract

*Simulating and forecasting the circulation of the global ocean is a difficult task. The circulation is forced at the surface by the atmosphere, but below the surface the circulation is dominated by internal nonlinear interactions. The kinetic energy in the ocean is dominated by mesoscale eddies, meanders and rings of the boundary currents with scales of 50 km to 500 km. Mesoscale eddies have a critical role in the dynamics of the ocean circulation with instabilities of the strong mean currents generating eddies in the upper-ocean, interactions between eddies transferring energy from the upper-ocean to the deep ocean, where eddies interact with bottom topography to generate abyssal mean-flows and eddies transferring momentum back to the mean currents. The present generation of high-resolution ocean circulation models, with horizontal resolution of  $\sim 1/10^\circ$ , appears to be deficient in kinetic energy when compared with long-term observations. A series of near-twin experiments, using the global HYbrid Coordinate Ocean Model (HYCOM) with identical atmospheric forcing, but varying in horizontal resolution and assimilation of altimetric steric height anomalies, show significant improvement with a better representation of mesoscale eddies when compared to observations from surface drifters, geostrophic currents from satellite altimetry, subsurface floats and deep current meter moorings. For a  $1/12.5^\circ$  ( $\sim 9$  km) global model, the eddy kinetic energy (EKE) at the surface and in the abyss is low by  $\sim 21\%$  and  $\sim 24\%$ , respectively, compared to surface drifting buoys and deep current meters. Increasing the model resolution to  $1/25^\circ$  ( $\sim 4.4$  km) or injecting mesoscale eddies through the assimilation of surface observations in a  $1/12.5^\circ$  model increases the surface and the abyssal EKE to levels consistent with the observations. In these models, the surface (abyssal) EKE is increased by 23% (51%) for the higher resolution model and 15% (46%) for the data-assimilative model. The upper-ocean kinetic energy of the mean-flow in the data-assimilative hindcast is decreased even though the surface and abyssal EKE are increased.*

### 1. Introduction

The eddy kinetic energy (EKE) in the upper-ocean, encompassed by mesoscale eddies, meanders and rings of the boundary currents [Stammer, 1997; Ferrari and Wunsch, 2009, 2010], is generated by instabilities of the mean flow and direct wind forcing. The present eddy-resolving global ocean general circulation models (OGCMs), running at  $\sim 1/10^\circ$  horizontal grid resolutions, appear to underestimate EKE at the surface compared to observations, indicating that the mean circulation is not inertial enough to generate vigorous upper-ocean instabilities, which in turn is responsible for the generation of meanders and eddies. Maltrud and McClean [2005] noted that eddy energy in the western boundary currents and relatively quiescent regions of the global  $1/10^\circ$  Parallel Ocean Program OGCM is too weak, when compared to sea surface height altimetry data. The eddy energy in the abyssal ocean is supplied by nonlinear interactions transferring energy from vertically-sheared baroclinic to depth-independent barotropic states [Rhines, 1979; Hurlburt and Hogan, 2008; Ferrari and Wunsch, 2009]. In the abyssal ocean, eddies interact with bottom topography to generate a strong eddy-driven mean circulation [Holland, 1978; Rhines, 1979].

Adequately representing mesoscale eddies and the energy and enstrophy cascades in ocean models is key to simulating the mean circulation with studies suggesting that horizontal resolutions around  $1/10^\circ$  are sufficient [Smith, et al., 2000; Hurlburt and Hogan, 2000; Oschlies, 2002; Maltrud and McClean, 2005]. However, at this resolution the models significantly underestimate the EKE in the abyssal ocean (depths greater than 3,000 m) [Scott, et al., 2010]. The eddy-driven mean abyssal circulation, which is constrained by the topography, can steer the mean pathways of the upper-ocean currents through a dynamical process known as upper-ocean - topographic coupling [Holland, 1978; Hogan and Hurlburt, 2000; Hurlburt, et al., 2008]. Recent model studies suggest that a strong eddy-driven mean abyssal circulation is sufficient to obtain a realistic Gulf Stream pathway and its separation from the western boundary [Hurlburt, et al., 2008]. Thus, a strong

abyssal circulation plays a critical role in the maintenance of mean circulation over the entire depth of the ocean, especially in regions dominated by intrinsic instability rather than atmospheric forcing. An intriguing question then becomes; how can we achieve a realistic representation of the abyssal ocean circulation in the OGCMs?

Resolution studies [Bryan, et al., 2007; Smith, et al., 2000; Hogan and Hurlburt, 2000; Oschlies, 2002] show that increasing the horizontal resolution for an OGCM generates a stronger mean-flow and thereby additional instabilities in the upper-ocean, which in turn can lead to a stronger eddy-driven abyssal circulation by vertically transferring the energy downward. Here we show that increasing the horizontal resolution from  $1/12.5^\circ$  to  $1/25^\circ$  yielded the most realistic representation of the ocean EKE from the surface to the abyss. Alternately, one can increase the EKE in the upper-ocean indirectly by injecting eddies via assimilating ocean surface observations in a  $1/12.5^\circ$  model. In this case, the additional EKE is generated by eddies introduced through data assimilation rather than intrinsic instability of the ocean dynamics. Our results indicate a significant increase in the abyssal ocean EKE when data assimilation is included. The major focus of attention in this paper is the comparative global ocean energetics from observations, employing four independent sets of observations representing the entire water column, and twin model experiments, only varying in horizontal resolution and data assimilation.

## 2. Model and Data

We present three model experiments differing only in horizontal resolution and data assimilation using the HYbrid Coordinate Ocean Model (HYCOM) [Bleck, 2002], which has 32 hybrid layers in the vertical and is forced with three-hourly,  $0.5^\circ$  Navy Operational Global Atmospheric Prediction System (NOGAPS) atmospheric fields. The models are a  $1/12.5^\circ$  ( $\sim 9$  km at the equator) and a  $1/25^\circ$  ( $\sim 4.4$  km at the equator) horizontal resolution non-assimilative models, denoted respectively as  $1/12.5^\circ$  FR and  $1/25^\circ$  FR and a  $1/12.5^\circ$  with data assimilation, denoted as  $1/12.5^\circ$  DA. The initial conditions for each experiment are spin-up from rest using the GDEM3 climatology for 10 years using climatological forcing. Thereafter, the model is forced with interannually varying NOGAPS atmospheric fields from 2003 to 2009. For the non-assimilative models, the analysis is performed for the five years 2005 to 2009. Only the two years, 2008–2009, are examined for the data-assimilative, where observations of satellite-derived sea surface height (SSH) and vertical profiles of temperature are incrementally inserted using a Multi-Variate Optimal Interpolation scheme [Cummings, 2005].

The modeled kinetic energy is compared to four independent sets of observations for three different dynamical regimes representing: 1) surface, 2) below the wind-driven mixed layer (150 m) and thermocline (1,000 m), and 3) abyssal ocean. At the surface, the instabilities of the mean-flow and direct-wind-forcing dominate, while quasi-geostrophy controls the energy below the mixed-layer and thermocline. We use kinetic energy estimates from surface drifter observations [Lumpkin and Pazos, 2007], satellite altimetry (150 m) [Ducet, et al., 2000], ARGO floats at 1,000 m [Lebedev, et al., 2007], and deep current moorings [Scott, et al., 2010] for model-data comparisons.

## 3. Results

At the surface, the highest EKE ( $>800 \text{ cm}^2 \text{ s}^{-2}$ ) are concentrated in the vicinity of the major current systems associated with the Gulf Stream and its continuation as the North Atlantic Current, the Loop Current in the Gulf of Mexico, the Brazil Current, the Kuroshio Current (off Japan), the equatorial current system and, in the southern hemisphere, the Antarctic Circumpolar Current (ACC), Agulhas Current (off southeast Africa), Eastern Australian Current, and Leeuwin Current near the western coast of Australia (Figure 1). The major circulation features, observed with the drifting buoys (Figure 1d), are reproduced by all models, as indicated by the high-spatial correlation ( $\sim 0.8$ ) between the model and observed EKE (Table 1). However, the global mean EKE differs significantly between the models and the observations, with  $1/25^\circ$  FR being the closest. Relative to the drifting buoys, the  $1/12.5^\circ$  FR model underestimates the global mean EKE by 21% (Table 1), implying weaker flow instabilities and fewer meanders. Increasing the model resolution increases the surface EKE by 23% from  $343 \text{ cm}^2 \text{ s}^{-2}$  in the  $1/12.5^\circ$  FR to  $423 \text{ cm}^2 \text{ s}^{-2}$  in  $1/25^\circ$  FR, which is 97% of the observed EKE ( $436 \text{ cm}^2 \text{ s}^{-2}$ ). The models are forced by identical atmospheric fields, which implies that the increase in EKE with resolution arises primarily from increased baroclinic and barotropic instability of the stronger mean-flow in the higher resolution model generating more meanders and eddies. Alternately, the increase in surface EKE could arise from a better representation of horizontal small-scale mixed-layer processes that are not resolved by the  $1/12.5^\circ$  model. Injecting eddies via assimilation of surface observations in the  $1/12.5^\circ$  DA experiment increases the surface EKE by 15% to  $393 \text{ cm}^2 \text{ s}^{-2}$ , which is 90% of the observed EKE. Thus, both the resolution and the data assimilation increase the overall global mean surface EKE by 23% and 15% respectively. There are, however, obvious model-data discrepancies of the spatial distribution of EKE in the simulations. For example, high-EKE, associated with the anti-cyclonic rings from the Agulhas Current (AC) at its

retroflexion, occurs along a narrow path in the non-assimilative simulations, but is not observed by the drifters nor the data-assimilative hindcast. The non-assimilative models tend to shed AC rings at regular intervals between the Agulhas Bank and Agulhas Plateau, and the rings travel northwestward into the South Atlantic with little dissipation. In the non-assimilative models, the AC is unable to penetrate into the Agulhas Basin. The erroneously large EKE along the wrong pathway is a known artifact of the model (also appears in other global models as well) and may be of the result of a too-strong AC, although the exact cause remains to be determined. For the global EKE statistics presented in Table 1 we excluded this region ( $20^{\circ}\text{W}$ - $10^{\circ}\text{E}$ ,  $40^{\circ}$ - $20^{\circ}\text{S}$ ). Exclusion of this region led to less than 5% changes in EKE at 150 m, and had a negligible contribution to the EKE at surface and depths below 1,000 m. Two other regions with significant departure from the observations occur off Java/Indonesia and in the Southeast Indian Ocean (seen only in  $1/25^{\circ}$  FR). Examination of altimeter-derived EKE in these regions shows similar patterns. Model-data differences in relatively quiescent regions (e.g., a bias toward lower-EKE in the southeast Pacific  $\sim 30^{\circ}\text{S}$ ) may be attributed, in part, to the shorter analysis period for the models (2005–2009) and to the atmospheric forcing. Compared to the drifting buoys the  $1/25^{\circ}$  FR model is too energetic in the high-EKE regions where intrinsic instability dominates the mesoscale eddies. In these highly-energetic regions, the estimated drifter EKE may be underestimated due to the tendency of the drifting buoys to accumulate in regions of weak flow.

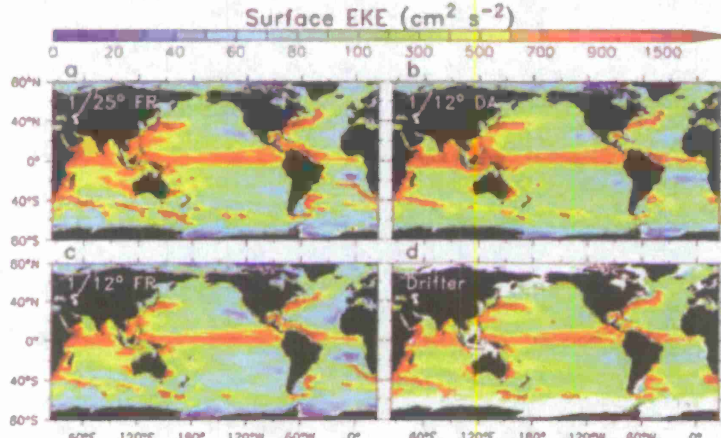


Figure 1. Surface-eddy kinetic energy (EKE in  $\text{cm}^2 \text{s}^{-2}$ ) from the three numerical experiments (a)  $1/25^{\circ}$  FR (2005–2009), (b)  $1/12.5^{\circ}$  DA (2008–2009), and (c)  $1/12.5^{\circ}$  FR (2005–2009) and (d) drifter observations encompassing the period 1983–2009. The surface drift observations are binned into  $1^{\circ} \times 1^{\circ}$  grids using daily values and those grid-points with at least 100 observations are considered. The EKE is computed from the daily velocity fields using the equation  $(\langle u'^2 \rangle + \langle v'^2 \rangle)/2$ , where brackets indicate time means and primes denote deviations from the time-mean velocities,  $(u', v') = (u, v) - (\langle u \rangle, \langle v \rangle)$ .

The kinetic energy of the mean flow (KEM) increases by 13% in the higher resolution simulation, from  $171 \text{ cm}^2 \text{s}^{-2}$  in  $1/12.5^{\circ}$  FR to  $193 \text{ cm}^2 \text{s}^{-2}$  in  $1/25^{\circ}$  FR. Associated with the stronger mean circulation is an increase in EKE. Over the entire ocean, a modest spatial correlation of  $\sim 0.67$  occurs between the model mean kinetic energy and the drifting buoy mean kinetic energy (Table 1). Visual inspection of the maps of KEM (not shown) exhibit arrow bands of high KEM ( $>700 \text{ cm}^2 \text{s}^{-2}$ ) coincident with the regions of high EKE indicating a stronger mean circulation with increased generation of meanders and eddies. The non-assimilative modeled KEM, however, is systematically higher than the drifter estimates by 21% and 42% respectively. The differences between the models and observations may arise from two possible sources; 1) drifting buoys tend to accumulate in regions of weak flow leading to a low bias in the mean-flow [Pasquero, et al., 2007] and 2) the analysis period for the models (2005–2009) is much shorter than the 22 years of buoy history. Injection of eddies by data assimilation increases the surface EKE, but the KEM is weaker in  $1/12.5^{\circ}$  DA compared to the non-assimilative simulations. Among the models, the spatial pattern of KEM in the  $1/12.5^{\circ}$  DA has a better correlation with the drifter observations, but a lower KEM of  $123 \text{ cm}^2 \text{s}^{-2}$  compared to the observed  $159 \text{ cm}^2 \text{s}^{-2}$ .

**Table 1. Observed and modeled eddy and mean kinetic energy. Abbreviations used: EKE, eddy kinetic energy; KEM, kinetic energy of mean-flow computed using the equation  $(\langle u^2 \rangle + \langle v^2 \rangle)/2$ , where brackets denote time means; FR, non-assimilative simulation; DA, data assimilative hindcast.**

| Model Expts.              | Surface <sup>a</sup>                                   |   | 150 m <sup>b</sup>                                     | 1000 m <sup>b</sup>                                    | Abyssal Ocean <sup>c</sup>                |   | Abyssal Ocean <sup>d</sup>                |   |
|---------------------------|--|---|--|--|---|---|---|---|
|                           | EKE <sup>e</sup><br>(cm <sup>2</sup> s <sup>-2</sup> ) | KEM<br>(cm <sup>2</sup> s <sup>-2</sup> ) | EKE <sup>e</sup><br>(cm <sup>2</sup> s <sup>-2</sup> ) | EKE <sup>e</sup><br>(cm <sup>2</sup> s <sup>-2</sup> ) | EKE<br>(cm <sup>2</sup> s <sup>-2</sup> ) | KEM<br>(cm <sup>2</sup> s <sup>-2</sup> ) | EKE<br>(cm <sup>2</sup> s <sup>-2</sup> ) | KEM<br>(cm <sup>2</sup> s <sup>-2</sup> ) |
| 1/12.5° FR<br>(2005–2009) | 343<br>(0.81)‡   | 171<br>(0.69)                             | 121<br>(0.64)  | 26.4<br>(0.77)   | 8.37                                      | 2.81                                      | 13.27<br>(0.71)                           | 6.84<br>(0.51)                            |
| 1/25° FR<br>(2005–09)     | 423<br>(0.82)  | 193<br>(0.67)                             | 181<br>(0.70)  | 37.9<br>(0.77)   | 12.61                                     | 4.44                                      | 18.28<br>(0.80)                           | 8.54<br>(0.54)                            |
| 1/12.5° DA<br>(2008–09)   | 393<br>(0.77)  | 160<br>(0.67)                             | 123<br>(0.79)  | 33.7<br>(0.71)   | 12.24                                     | 3.48                                      | 14.17<br>(0.80)                           | 6.83<br>(0.33)                            |
| Obs.                      | 436  | 135                                       | 159  | 27.5   |   |   | 17.73                                     | 8.21                                      |

<sup>a</sup>Mean over the global ocean (70°S–70°N)

<sup>b</sup>Mean over the global ocean (60°S–60°N) excluding the tropical ocean (5°S–5°N) where the assumption of geostrophy leads to potentially large errors

<sup>c</sup>Mean over the global ocean (70°S–70°N) using 3°×3° grid

<sup>d</sup>Due to the unrealistic Agulhas overshooting into the south Atlantic in the simulations, the region bounded by 20°W–10°E, 40°–20°S is excluded from mean.

<sup>e</sup>Mean values obtained at the 712 current meter mooring locations

<sup>‡</sup>The spatial correlation coefficient between the model and observed kinetic energy

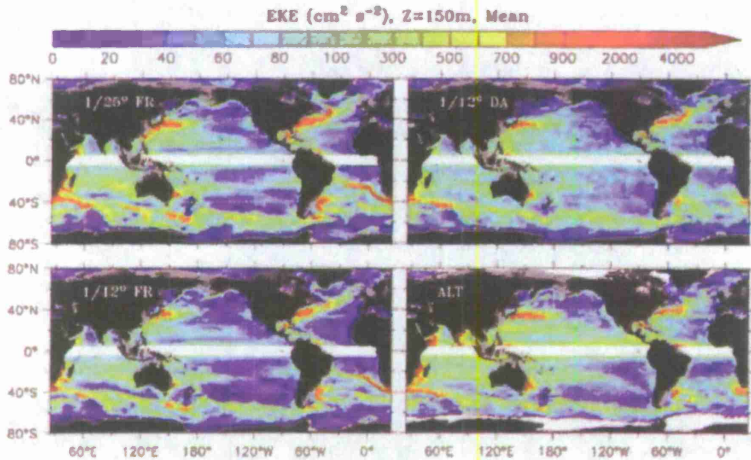


**Figure 2. Eddy kinetic energy (EKE in cm<sup>2</sup> s<sup>-2</sup>) at 150m from the three numerical experiments (a) 1/25° FR (2005–2009), (b) 1/12.5° DA (2008–2009), and (c) 1/12.5° FR (2005–2009) and (d) geostrophic velocity estimates from AVISO sea surface height maps for the period 2005–2009. The band 5°N to 5°S is excluded from the EKE estimates.**

Quasi-geostrophic flow dominates the EKE below the wind-driven mixed layer. In Table 1 and Figure 2, the EKE of the models at 150 m is compared with geostrophic velocity estimates from mapped satellite altimeter sea surface heights (SSH) [Ducet, et al., 2000]. At 150 m, which is below the wind-driven mixed layer, but still representative of the upper-ocean, the EKE of the 1/25° FR is the highest at 181 cm<sup>2</sup> s<sup>-2</sup> exceeding the altimeter estimate by 14%. Both 1/12.5° FR and 1/12.5° DA have nearly the same EKE (122 cm<sup>2</sup> s<sup>-2</sup>) approximately 23% below the altimeter estimate (159 cm<sup>2</sup> s<sup>-2</sup>). The 1/12.5° models rapidly attenuate the EKE with depth which makes a quantitative comparison with the surface geostrophic velocity difficult. Among the models, 1/12.5° DA is highly correlated with the altimeter EKE with a correlation coefficient of 0.79. We expect the energy estimates from the SSH are affected by sampling artifacts. The mapped geostrophic velocity estimates will be lower than the true geostrophic velocity due to the removal of variability on times shorter than approximately 10 days and horizontal scales smaller than approximately 50 km.

Within the lower thermocline we use subsurface drift vectors at 1,000 m from the ARGO floats [Lebedev, et al., 2007] to examine the EKE. Again, the energy estimates from the ARGO float are subjected to sampling errors. The number of ARGO floats is much smaller than the number of surface drifters. For the past 5 years, approximately 3,000 ARGO floats return a position observation every 10 days. Thus, the sampling of the ARGO floats is coarser in space and time with a

shorter history than surface drifters. We have binned the drift vectors on a  $3^\circ \times 3^\circ$  grid to get at least 100 observations in each grid box. Given the small sample size, we expect the ARGO EKE estimates to be biased low. At 1,000 m, the higher resolution and data assimilative model EKE exceed the  $1/12.5^\circ$  FR by 44% (26.4 to  $37.9 \text{ cm}^2 \text{ s}^{-2}$ ) and 28% (26.4 to  $33.7 \text{ cm}^2 \text{ s}^{-2}$ ) respectively, similar to the surface EKE (Table 1). The  $1/12.5^\circ$  FR underestimates the observed EKE by 4%. Eddies in the upper-ocean have a significant impact on the abyssal circulation (depths greater than 3,000 m), as abyssal currents can be generated by baroclinically-unstable flows via vertical transfer of eddy energy into the abyssal ocean. In the models, high-abyssal ocean EKE ( $80\text{--}300 \text{ cm}^2 \text{ s}^{-2}$ ) is confined to the regions below high-surface EKE such as western boundary currents and the ACC (Figure 2), a strong indicator of vertical transfer of EKE from the surface to the abyssal ocean. For the global abyssal ocean, the EKE increases by 51% from  $8.4 \text{ cm}^2 \text{ s}^{-2}$  to  $12.6 \text{ cm}^2 \text{ s}^{-2}$  when the resolution is doubled, and by 46% to  $12.2 \text{ cm}^2 \text{ s}^{-2}$  with data assimilation (Table 1). In the  $1/12.5^\circ$  DA, the surface eddies introduced by the assimilation of sea surface height are driving a stronger eddy-driven abyssal circulation. The SSH anomalies are converted into synthetic profiles of temperature and salinity in the upper-ocean for assimilation. A comparison of model EKE with a global dataset of 712 quality-controlled moored current meter records [Scott, et al., 2010] indicates that the  $1/25^\circ$  FR has the most realistic representation of abyssal ocean EKE and the  $1/12.5^\circ$  FR underestimates the EKE by 24%. At these locations, the EKE increased from  $13.3 \text{ cm}^2 \text{ s}^{-2}$  in  $1/12.5^\circ$  FR to  $18.5 \text{ cm}^2 \text{ s}^{-2}$  in the  $1/25^\circ$  FR, comparable with the observed current meter measurements ( $17.5 \text{ cm}^2 \text{ s}^{-2}$ , Table 1). When correlated with the current meter observations, both  $1/25^\circ$  FR and  $1/12.5^\circ$  DA EKE has higher correlation ( $\sim 0.8$ ) compared to  $1/12.5^\circ$  FR (0.71). For the mean global abyssal circulation, the KEM increases by 58% for  $1/25^\circ$  FR and 24% with data assimilation. However, at the current meter locations the KEM increases by 25% with the doubled resolution, but remains virtually unchanged with data assimilation.

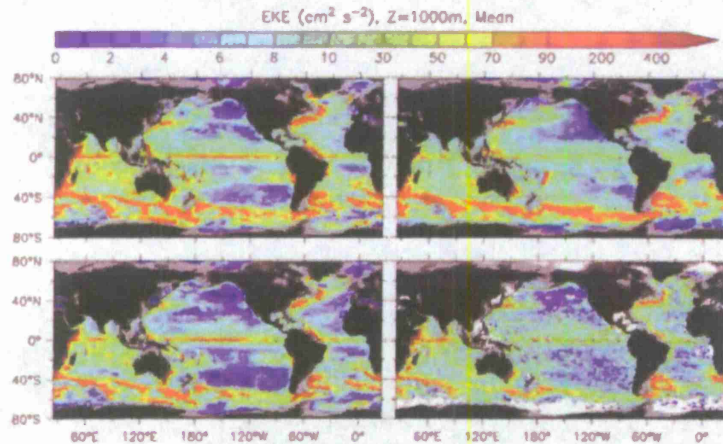


Figure 3. Eddy kinetic energy (EKE in  $\text{cm}^2 \text{ s}^{-2}$ ) at 1,000m from the three numerical experiments (a)  $1/25^\circ$  FR (2005–2009), (b)  $1/12.5^\circ$  DA (2008–2009), and (c)  $1/12.5^\circ$  FR (2005–2009) and (d) ARGO 1,000m drift observations encompassing the period 1998–2009. The surface drift observations are binned into  $3^\circ \times 3^\circ$  grids using daily values and those grid points with at least 100 observations are considered.

Noting that the abyssal EKE is greatest beneath the regions of high-surface EKE, we have extracted the Gulf Stream region ( $80^\circ\text{W}\text{--}30^\circ\text{W}$ ,  $10^\circ\text{N}\text{--}60^\circ\text{N}$ ) for closer examination. The overall patterns of surface EKE in both  $1/12.5^\circ$  DA and  $1/25^\circ$  FR are similar to the drifter observations (Figures 3a–3d). In  $1/12.5^\circ$  FR, the simulated EKE along the North Atlantic Current between  $55^\circ\text{W}$  and  $35^\circ\text{W}$  is significantly underestimated (see box in Figures 3a–3d). In the abyssal ocean, it is clear from the superimposed current meter observations in Figures 3e–3g that both the double-resolution and data assimilative models have realistic EKE below the Gulf Stream. The  $1/12.5^\circ$  FR EKE is too low east of  $60^\circ\text{W}$ , typically by a factor of two and too weak farther to the west consistent with the weaker surface EKE.

#### 4. Conclusion

The surface and abyssal circulation of the ocean are strongly coupled through the cascades that vertically redistribute the energy and vorticity throughout the entire water column. The surface kinetic energy of ocean circulation is dominated by eddy kinetic energy (EKE) associated with the instabilities of the mean-flow and direct wind forcing. The eddy-eddy interactions transfer energy, initially, from large scales towards the Rossby radius scale and vorticity towards small scales.

At scales near the Rossby radius, energy is transferred from the upper- ocean into the abyss (barotropification). The abyssal-eddies interact with topography and can transfer energy back to the mean-flow. The present generation of eddy-resolving global ocean circulation models at  $\sim 1/10^\circ$  resolution appear to underestimate the EKE in both the upper and abyssal ocean. For example, the simulated EKE in a  $1/12.5^\circ$  FR accounts for only about 79% and 76% of the observations at the surface and at the abyssal ocean respectively. We show that doubling the model resolution ( $1/25^\circ$ ) to better resolve the nonlinear eddy cascades of energy and enstrophy or by injecting eddies via assimilating ocean surface observations improves the model energetics to be consistent with independent observations over most of the world's oceans. An increase in the surface EKE by 23% (15%) and the corresponding 51% (46%) increase in the abyssal EKE in the  $1/25^\circ$  FR ( $1/12.5^\circ$  DA) model clearly demonstrates the need to improve representation of upper-ocean EKE as a prerequisite for strong eddy-driven abyssal circulation. The surprising result from these experiments is the impact of a modest increase in resolution on the energetic of the eddy-resolving OGCM. While the models examined clearly resolve the Rossby radius (dominant-eddy scale), the model dynamics require resolving the eddy-eddy interactions and the cascades of energy and enstrophy. Vorticity and enstrophy are dominated by smaller horizontal scales and benefit from the increased resolution.

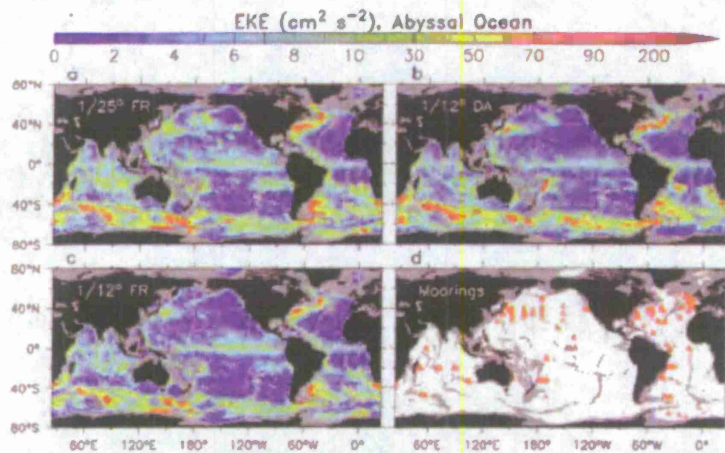


Figure 4. Abyssal ocean EKE ( $\text{cm}^2 \text{ s}^{-2}$ ) averaged below 3,000 m from the three numerical experiments (a)  $1/25^\circ$  FR, (b)  $1/12.5^\circ$  DA, (c)  $1/12.5^\circ$  FR and (d) locations of the 712 deep current meter moorings used to validate the model kinetic energy [see Scott, et al., for details]. Moorings with a record at least 180 days are considered. Depths less than 3,000 m are masked grey.

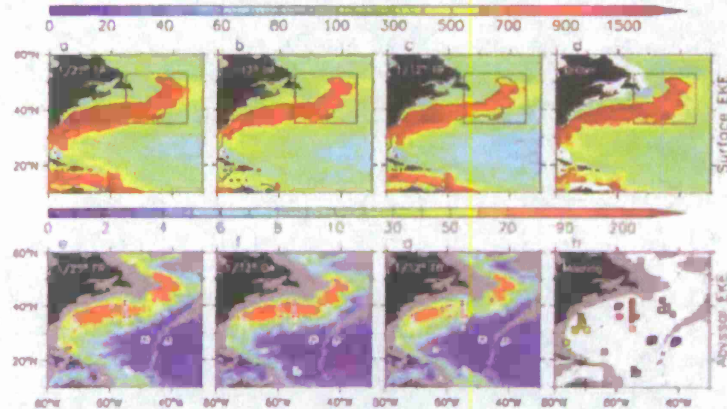


Figure 5. The EKE in the Gulf Stream region. Surface EKE ( $\text{cm}^2 \text{ s}^{-2}$ ) for the three numerical experiments (a)  $1/25^\circ$  FR, (b)  $1/12.5^\circ$  DA, and (c)  $1/12.5^\circ$  FR with the  $800 \text{ cm}^2 \text{ s}^{-2}$  contour from the (d) drifter observations superimposed on the model surface EKE. Abyssal ocean EKE ( $\text{cm}^2 \text{ s}^{-2}$ ) averaged below 3,000 m for the Gulf Stream region from the three numerical experiments (e)  $1/25^\circ$  FR, (f)  $1/12.5^\circ$  DA, and (g)  $1/12.5^\circ$  FR with superimposed EKE estimates from the (h) moored current meter observations shown as color-filled squares (same color shading for both models and the observations). Depths less than 3,000 m are masked grey.

## Acknowledgements

This work was supported in part by a grant of computer time from the DoD High Performance Computing Modernization Program at the NAVY DoD Supercomputing Resource Center (DSRC). It was sponsored by the Office of Naval Research (ONR) through the NRL projects, Eddy-Resolving Global Ocean Prediction Including Tides and Ageostrophic Vorticity Dynamics of the Ocean. We thank Robert Scott of the Université de Bretagne Occidentale for providing the historical current meter data and E. Joseph Metzger, Ole Martin Smedstad, and Luis Zamudio (NRL) for making the global HYCOM simulations available.

## References

Bleck, R., "An oceanic general circulation model framed in hybrid isopycnic-cartesian coordinates", *Ocean Modell.*, 4, pp. 55–88, 2002.

Bryan, F.O., M.W. Hecht, and R.D. Smith, "Resolution convergence and sensitivity studies with North Atlantic circulation models. Part I: The western boundary current system", *Ocean Modell.*, 16, pp. 141–159, 2007.

Cummings, J.A., "Operational multivariate ocean data assimilation", *Q. J. Roy. Meteorol. Soc.*, 131, pp. 3583–3604, 2005.

Ducet, N., P.-Y. Le Traon, and G. Reverdin, "Global high-resolution mapping of ocean circulation from TOPEX/Poseidon and ERS-1 and 2", *J. Geophys. Res.*, 105, pp. 19477–19498, 2000.

Ferrari, R. and C. Wunsch, "Ocean circulation, kinetic energy: reservoirs, sources and sinks", *Annu. Rev. Fluid Mech.*, 41, pp. 253–282, 2009.

Ferrari, R. and C. Wunsch, "The distribution of eddy kinetic and potential energies in the global ocean", *Tellus*, 62A, pp. 92–108, 2010.

Hogan, P.J. and H.E. Hurlburt, "Impact of upper-ocean - topographic coupling and isopycnal outcropping in Japan/East Sea models with 1/8° to 1/64° resolution", *J. Phys. Oceanogr.*, 30, pp. 2535–2561, 2000.

Holland, W.R., "The role of mesoscale eddies in the general circulation of the ocean - numerical experiments using a wind-driven quasi-geostrophic model", *J. Phys. Oceanogr.*, 8, pp. 363–392, 1978.

Hurlburt, H.E., and P.J. Hogan, "Impact of 1/8° to 1/64° resolution on Gulf Stream model-data comparisons in basin-scale subtropical Atlantic ocean models", *Dyn. Atmos. Oceans.*, 32, pp. 283–329, 2000.

Hurlburt, H.E. and P.J. Hogan, "The Gulf Stream pathway and the impacts of the eddy-driven abyssal circulation and the deep western boundary current", *Dyn. Atmos. Oceans.*, 45, pp. 71–101, 2008.

Hurlburt, H.E., E.J. Metzger, P.J. Hogan, C.E. Tilburg, and J.F. Shriver, "Steering of upper-ocean currents and fronts by the topographically-constrained abyssal circulation", *Dyn. Atmos. Oceans.*, 45, pp. 102–134, 2008.

Lebedev, K.V., H. Yoshinari, N.A. Maximenko, and P.W. Hacker, "Velocity data assessed from trajectories of Argo floats at parking level and at the sea surface", *IPRC Technical Note No. 4(2)*, Honolulu, HI, 16pp, 2007.

Lumpkin, R. and M. Pazos, "Measuring surface currents with Surface Velocity Program drifters: the instrument, its data, and some recent results", *Lagrangian Analysis and Prediction of Coastal and Ocean Dynamics*, A. Griffa, A.J. Mariano, A.D. Kirwan, T. Ozgokmen, and H.T. Rossby (editors), Cambridge Univ. Press, Cambridge, pp. 39–67, 2007.

Maltrud, M.E. and J.L. McClean, "An eddy-resolving global 1/10° ocean simulation", *Ocean Modell.*, 8, pp. 31–54, 2005.

Oschlies, A., "Improved representation of upper-ocean dynamics and mixed-layer depths in a model of the North Atlantic on switching from eddy-permitting to eddy-resolving grid resolution", *J. Phys. Oceanogr.*, 32, pp. 2277–2298, 2002.

Pasquero, C., A. Bracco, A. Provenzale, and J.B. Weiss, "Particle motion in a sea of eddies", *Lagrangian Analysis and Prediction of Coastal and Ocean Dynamics*, A. Griffa, A.J. Mariano, A.D. Kirwan, T. Ozgokmen, and H.T. Rossby (editors), Cambridge Univ. Press, Cambridge, pp. 89–118, 2007.

Rhines, P.B., "Geostrophic turbulence", *Ann. Rev. Fluid Mech.*, 11, pp. 401–440, 1979.

Scott, R.B., B.K. Arbic, E.P. Chassignet, A.C. Coward, M. Maltrud, W.J. Merryfield, A. Srinivasan, and A. Varghese, "Total kinetic energy in four global eddying ocean circulation models and over 5000 current meter records", *Ocean Modell.*, 32, pp. 157–169, 2010.

Smith, R.D., M. Maltrud, F.O. Bryan, and M.W. Hecht, "Numerical simulation of the North Atlantic Ocean at 1/10°", *J. Phys. Oceanogr.*, 30, pp. 1532–1561, 2000.

Stammer, D., "Global characteristics of ocean variability estimated from regional TOPEX/Poseidon altimeter measurements", *J. Phys. Oceanogr.*, 27, pp. 1743–1769, 1997.